A Series Interharmonic Filter for Cascaded H-bridge PV Inverters

Pan, Yiwei; Sangwongwanich, Ariya; Yang, Yongheng; Blaabjerg, Frede

Published in:
Proceeding of 2020 IEEE Energy Conversion Congress and Exposition (ECCE)

DOI (link to publication from Publisher):
10.1109/ECCE44975.2020.9235745

Publication date:
2020

Document Version
Accepted author manuscript, peer reviewed version

A Series Interharmonic Filter for Cascaded H-bridge PV Inverters

Yiwei Pan, Ariya Sangwongwanich, Yongheng Yang, and Frede Blaabjerg
Department of Energy Technology, Aalborg University
Pontoppidanstraede 111, Aalborg 9220, Denmark
E-mails: {ypa, ars, yoy, fbl}@et.aau.dk

***Abstract*—Interharmonics have become one of the challenging issues in photovoltaic (PV) systems. One of the reasons for interharmonic emissions is the maximum power point tracking (MPPT) control. In cascaded H-bridge (CHB) PV inverters, due to the potential superposition of the MPPT perturbations of individual PV cells, a higher oscillation may appear in the equivalent total DC voltage, leading to large interharmonics in the grid. To mitigate the interharmonics from CHB PV inverters, a series interharmonic filter is proposed in this paper, which employs a series H-bridge cell as an active filter. With the proposed control, the equivalent DC voltage can be maintained oscillation-free, thereby suppressing the interharmonics. In practice, the interharmonic filter can be either an additional unit, or a redundant cell in the cascaded PV converter. Simulations and experimental results have validated the effectiveness of the proposed solution.**

***Keywords*—Cascaded H-bridge (CHB), interharmonics, maximum power point tracking (MPPT), photovoltaic (PV) systems, power quality.**

I. INTRODUCTION

Interharmonics are defined as harmonic components with their frequencies being non-integer times of the fundamental frequency, which may cause voltage fluctuation, flickering, unintentional tripping of the protection circuit, etc [1]. In the past decades, with the fast growing penetration of photovoltaic (PV) systems and other power electronics equipment, the interharmonic issue has become much severer than ever before. According to IEEE Standard 1547-2018 and IEC TS 63102, interharmonics are one of the assessment criteria for grid-connected PV systems [2], [3]. In the prior-art investigation, it has been revealed that the maximum power point tracking (MPPT) perturbation is possibly responsible for interharmonic emissions in PV systems [4], [5]. It can be further explained as follows: the MPPT perturbation will induce low frequency oscillations on the DC voltage of the PV inverter, and after the convolution with the grid frequency through the control loops, interharmonics are generated in the grid current [5], [6].

To mitigate interharmonics from conventional two-level PV inverters, an adaptive gain method and a rate limiter method have been introduced in [7]. By avoiding the abrupt change on the amplitude of the current reference, interharmonics can be effectively reduced. However, the suppression performances are not significant. In [8], a random sampling rate MPPT has been developed, which is capable to suppress the interharmonics to a large extent. Nevertheless, its mitigation capability is limited, because this method is not able to fully eliminate the MPPT perturbation, which is the main source of interharmonics, as aforementioned.

On the other hand, the cascaded H-bridge (CHB) converter concept has been introduced to PV applications owing to its modularity, high output power quality, and high efficiency [9], [10]. However, due to the potential superposition of the MPPT perturbation on the DC voltages of individual CHB cells, interharmonics from CHB PV inverters could be larger than an individual PV inverter. In the worst case, the interharmonics can be n-times larger than one single PV inverter (n denotes the number of the cascaded cells), if the DC-side oscillations of the CHB cells are in-phase [11]. Therefore, the interharmonic issue is much severer and more complex in CHB PV inverters than two-level PV inverters. To address the harmonic/interharmonic issue in CHB converters, in [12], a DC-link ripple feedforward compensation method has been proposed. Although it is effective to reject low-order harmonics, this method is not capable to suppress interharmonics caused by the MPPT control. Recently, a phase-shifting MPPT (PS-MPPT) method has been proposed in [11] and [13]. By properly shifting the phases of the DC voltage oscillations, the interharmonics can be mitigated. However, interharmonics may still become larger under varying environmental conditions, since the MPPT oscillation may not be properly phase-shifted in operation [14]. In [13] and [14], the interharmonic mitigation performance of the random sampling-rate MPPT method for CHB PV inverters has been further studied, where it has been revealed that this method is more suitable for applications with a large cascading number (i.e., n should be large). Nevertheless, more attempts should be made to tackle the interharmonic issue in CHB PV inverters.

Despite the interharmonic amplification issue, the multi-module structure of the CHB inverter has provided more control flexibilities in enhancing the output power quality and managing harmonics. For instance, in [15], A series PV-battery-hybrid system has been proposed, where batteries have been integrated in some cells of the CHB PV inverter to compensate the fluctuation of the PV power. In [16] and [17], low-order harmonics were utilized by some cells to broaden the operational range of the CHB inverter, while some other cells were selected to operate as active filters. Considering the above, a series interharmonic filter is proposed in this paper for CHB PV inverters. A series H-bridge cell only with capacitors on its DC side is employed as the interharmonic filter. With a two-layer control, the series H-bridge cell will effectively damp interharmonics from other PV converter cells. The oscillation

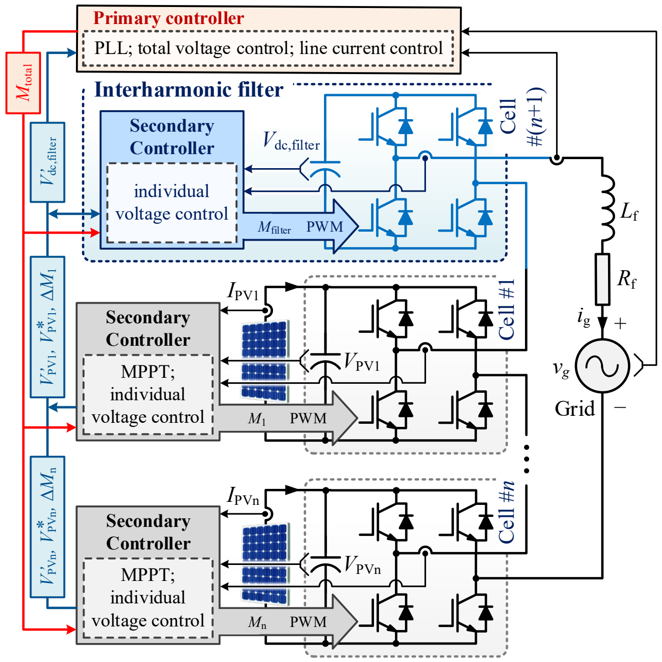

Fig. 1. Overall diagram of a single-phase CHB PV inverter with the proposed series interharmonic filter (PWM – pulse width modulation; PLL – phase locked loop), where I_{PVk} and V_{PVk} denote the PV current and voltage of the k^{th} cell, $V_{\mathrm{dc,filter}}$ is the DC voltage for the interharmonic filter, L_{f} and R_{f} represent the impedance of the output filter, and v_{g} and i_{g} are the grid voltage and current, respectively.

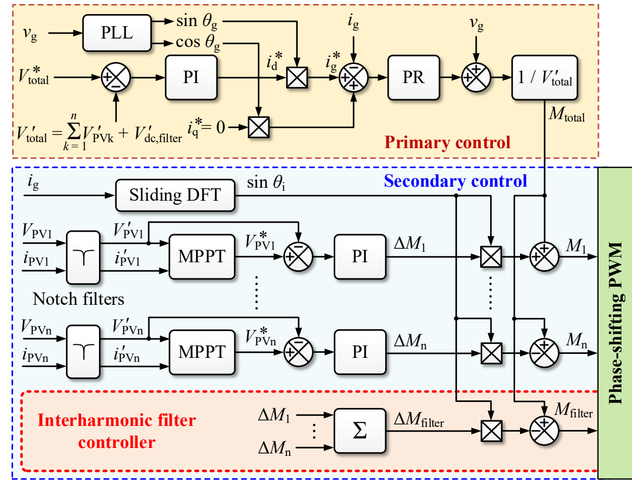

Fig. 2. Control diagram of a single-phase CHB PV inverter with the proposed series interharmonic filter (DFT – discrete Fourier transform; PR – proportional resonant).

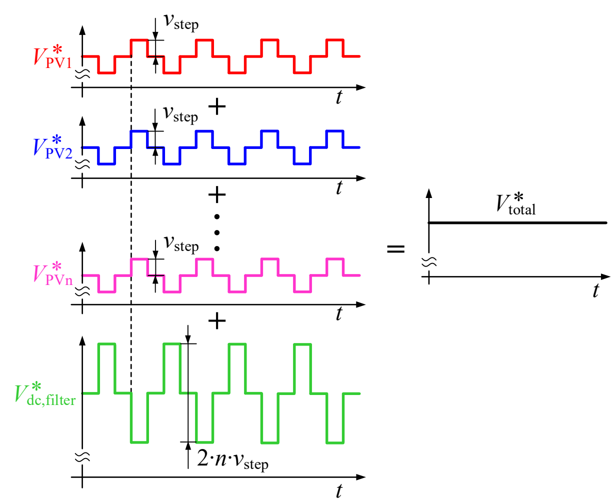

Fig. 3. DC voltage references of a CHB PV inverter with n PV converter cells and an interharmonic filter cell, where $V^*_{\mathrm{dc,filter}}$ denotes for the equivalent DC voltage reference for the interharmonic filter.

on the equivalent total DC voltage can be suppressed, and thereby, mitigating the interharmonics. In practice, the added interharmonic filter can also be reserved as a redundant cell to increase the reliability of the CHB PV system. The effectiveness of the proposed method is verified by both simulation and experimental results.

II. Proposed Series Interharmonic Filter

The configuration of the proposed series interharmonic filter is shown in Fig. 1, where an H-bridge cell only with capacitors on its DC side is in series with n PV converter cells, and operates as the interharmonic filter. A two-layer control structure is adopted in the system, where the primary control is responsible for the grid current regulation and total DC voltage control, and the secondary control is in charge of the individual voltage control. With this, the control system can be either centralized or decentralized [9], [10]. For the decentralized control, the low-bandwidth communication system (LBC) is necessary [9].

The detailed control diagram of the system is shown in Fig. 2. As it is observed in Fig. 2, the primary control gathers the filtered DC voltages V'_{PVk}, $V'_{\mathrm{dc,filter}}$ (k denotes the index of CHB cells, and $V'_{\mathrm{dc,filter}}$ is the filtered DC voltage of the interharmonic filter) and the PV voltage reference V^*_{PVk} from the secondary controllers, and regulates the sum of the DC voltages through a voltage/current dual-loop control. The generated modulation index M_{total} is then equally distributed to each converter cell. In the secondary control, the PV voltages are regulated by proportional-integral (PI) controllers according to the voltage reference generated by the distributed MPPT controllers, and a set of modified values for the modulation index M_{total}, denoted by ΔM_{k}, are generated. For the k^{th} PV converter cell, the modulation index can be calculated as

$$M_{\mathrm{k}} = M_{\mathrm{total}} + \Delta M_{\mathrm{k}} \sin\theta_{\mathrm{i}} \tag{1}$$

where θ_{i} is the phase angle of the grid current i_{g}, which can be calculated by sliding discrete Fourier transform (SDFT) algorithm [18]. When the reactive current reference i^*_{q} equals to zero, θ_{i} equals to the phase angle of the grid voltage θ_{g}. For the series interharmonic filter, its modulation index M_{filter} can then be determined as

$$M_{\mathrm{filter}} = M_{\mathrm{total}} - \left(\sum_{k=1}^{n} \Delta M_{\mathrm{k}}\right)\sin\theta_{\mathrm{i}} \tag{2}$$

Since the oscillation on the equivalent total DC voltage is primarily responsible for the interharmonic emissions, the

TABLE I
PARAMETERS OF THE CHB PV INVERTER.

Rated power for one PV module	1066 W
DC capacitance for each CHB cell	680 μF
Grid-side *L*-filter	5.4 mH
Switching frequency of the cells	10 kHz
Controller sampling frequency	10 kHz
Grid voltage (RMS)	220 V
Grid frequency	50 Hz
MPPT sampling rate	10 Hz
MPPT step-size	5 V

reference of the total DC voltage V^*_{total} should be constant. In this case, the DC voltage of the interharmonic filter should oscillate in a way to counteract with the sum of the DC voltage oscillations of all other cells. Considering the worst case where the DC voltages of PV converter cells oscillate in phase, the DC voltage of the interharmonic filter should be at least larger than $2 \cdot n \cdot v_{step}$, as illustrated in Fig. 3, where v_{step} stands for the MPPT step-size. However, in practice, V^*_{total} should be set higher to accommodate higher voltage variations, which may occur during the irradiance change.

In terms of implementation, the interharmonic filter cell can be manually added in hardware. In addition to its functionality in interharmonic suppression, this added converter cell can be reserved as one redundant cell to improve the reliability of the entire system (e.g., by circulating reactive power flow) [19]. On the other hand, the interharmonic filter cell can also be selected among the existing PV converter cells, and the preferred choice should be the one with the minimum power contribution. That is, one PV converter may be in idle mode due to uneven shading, and then, this cell can be selected as the interharmonic filter with negligible active power contribution. In this way, although a certain amount of solar energy is discarded, it is acceptable as the discarded power is minimized, while the overall power quality of the delivered power is improved.

III. SIMULATION AND EXPERIMENTAL RESULTS

A. Simulation Results

To validate the effectiveness of the proposed interharmonic filter, simulations are performed on a 3-cell CHB PV inverter. The system parameters are shown in Table I and the simulation results are shown in Figs. 4 − 7.

Firstly, two cases are used to demonstrate the interharmonic performance of the CHB PV inverter. As shown in Fig. 4, the DC voltages of all PV converter cells oscillate in phase. Consequently, the equivalent total DC voltage oscillates with an amplitude of 15 V, which is three times higher than one single converter cell. As a result, large interharmonics appear with the frequency being $50 \pm (2m+1) / (4T_{MPPT})$, where $m = 0$, 1, 2…, and the amplitudes of almost all the main harmonics within 0 − 100 Hz are larger than 0.1 A. On the other hand, as shown in Fig. 5, when the DC oscillations of CHB cells are shifted by T_{MPPT}, the oscillation of the equivalent total DC voltage is around 5 V. Hence, the interharmonics in the grid current are also reduced, with the amplitudes of the main

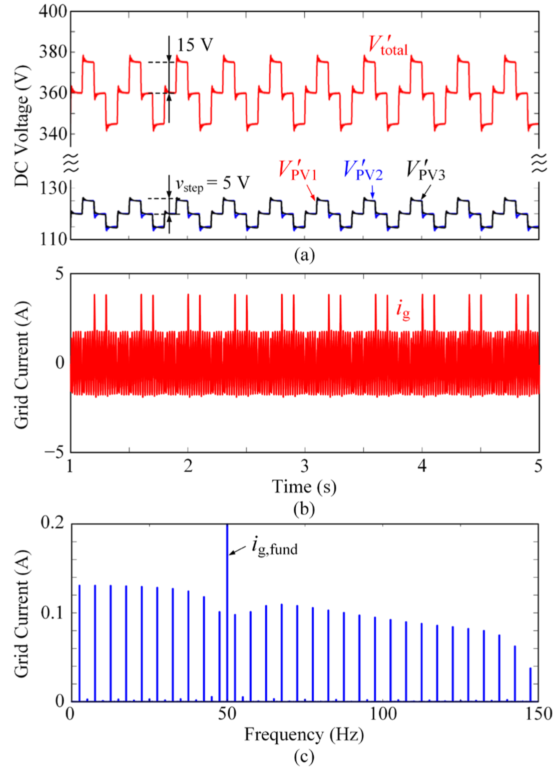

Fig. 4. Simulation results of a 3-cell CHB PV inverter with in-phase oscillation of DC voltages ($i_{g,fund}$ denotes the fundamental component of the grid current): (a) DC voltages of 3 CHB cells and the equivalent total DC voltage, (b) grid current, and (c) frequency spectrum of the grid current.

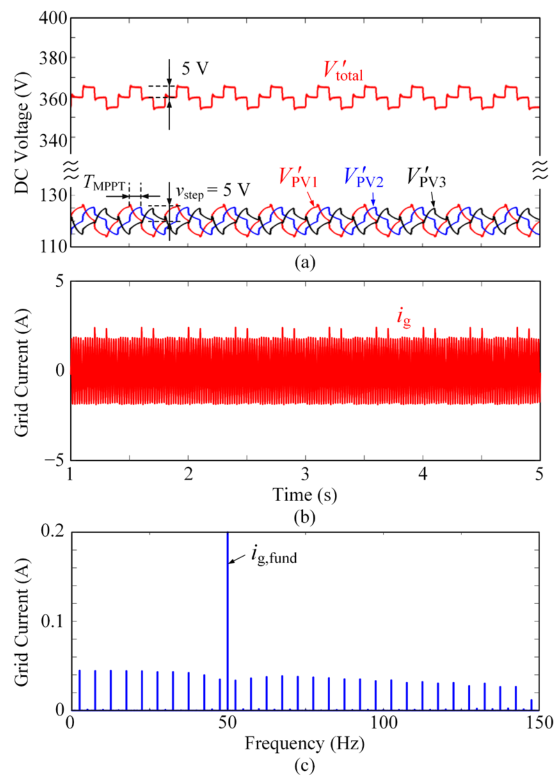

Fig. 5. Simulation results of a 3-cell CHB PV inverter with DC voltage oscillations shifted by T_{MPPT} (PS-MPPT): (a) DC voltages of 3 CHB cells and the equivalent total DC voltage, (b) grid current, and (c) frequency spectrum of the grid current.

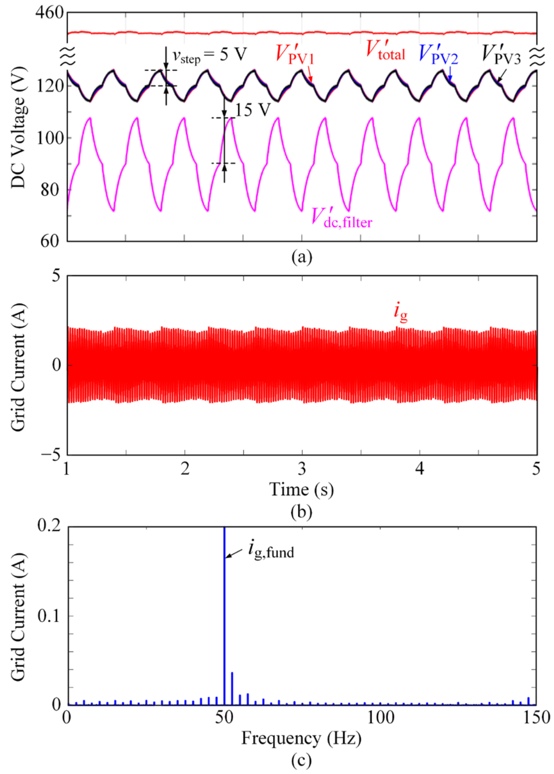

Fig. 6. Performance of the series interharmonic filter with a 3-cell CHB PV inverter, where the DC voltages of PV converter cells oscillate in phase: (a) DC voltages, (b) grid current, and (c) frequency spectrum of the grid current.

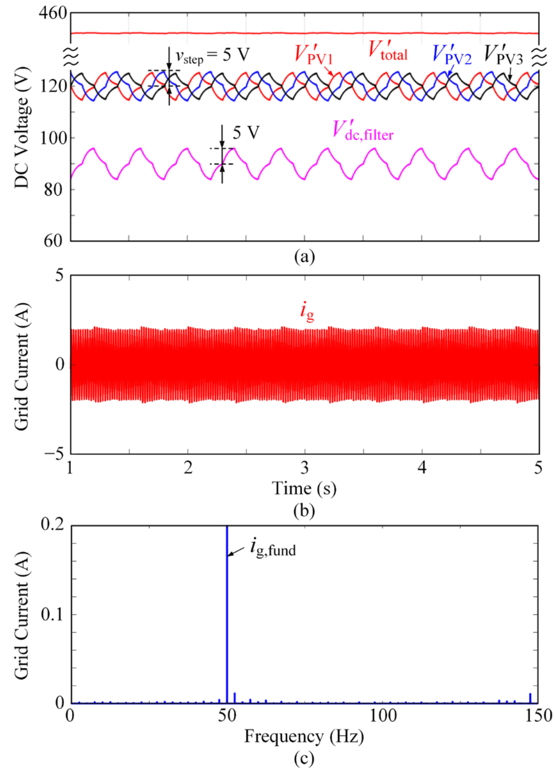

Fig. 7. Performance of the series interharmonic filter with a 3-cell CHB PV inverter, where the DC voltage oscillations of PV converter cells are shifted by T_{MPPT}: (a) DC voltages, (b) grid current, and (c) frequency spectrum of the grid current.

interharmonics being around 0.04 A, which is approximately one third comparing to the case in Fig. 4. The phases of the DC voltage oscillations are usually randomly determined in practice, but it can be realized by employing the PS-MPPT proposed in [13]. However, the PS-MPPT is more effective in steady-state conditions. Under varying environmental conditions, such as the slow change of irradiance and temperature, it may not be able to keep all the DC voltages properly phase-shifted. Interharmonics may increase in such cases [14]. Moreover, the PS-MPPT has a limited interharmonic suppression performance when an odd number of cells are cascaded, as exemplified in Fig. 5, where interharmonics are still relatively large with a variety of frequencies.

The above two cases are then tested with the proposed series interharmonic filter. An additional H-bridge converter is inserted in series with the 3-cell CHB PV inverter, with its parameters being identical to the other CHB cells. The total DC voltage reference is raised to 450 V, due to the insertion of the additional filter cell. As shown in Fig. 6, for the in-phase oscillation case, a reversed oscillating DC voltage with an amplitude of 15 V is generated by the interharmonic filter. Consequently, the oscillation on the total DC voltage is minimized, and the interharmonics in the grid current are significantly suppressed, as shown in Fig. 6(c). As further observed in the frequency spectrum in Fig. 6(c), except for the interharmonics at 52.5 Hz, whose amplitude is only 0.036 A, all the other interharmonics are suppressed below 0.015 A. For the case with shifted DC voltage oscillations, the interharmonic

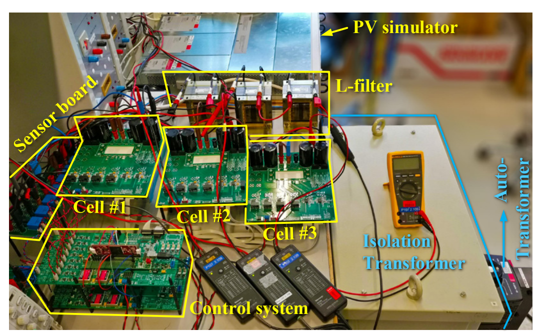

Fig. 8. Photo of the experiment setup with two PV converter cells and one interharmonic filter cell.

performance is further improved with the proposed interharmonic filter. As shown in Fig. 7, a 5-V oscillating voltage is generated by the interharmonic filter on its DC voltage to cancel the low-frequency oscillation induced by PV converter cells, and the total DC voltage is almost constant. Therefore, due to the lowered DC voltage perturbation, a much better interharmonic performance is achieved, as shown in Fig. 7(c), where almost all interharmonics are eliminated, except for interharmonic components at 52.5 Hz and 147.5 Hz, with their amplitudes being only 0.01 A. Therefore, the interharmonics from the CHB PV inverters can be effectively suppressed by the proposed series interharmonic filter.

According to the frequency spectra shown in Figs. 6(c) and 7(c), it is clear that the interharmonic filter performs better

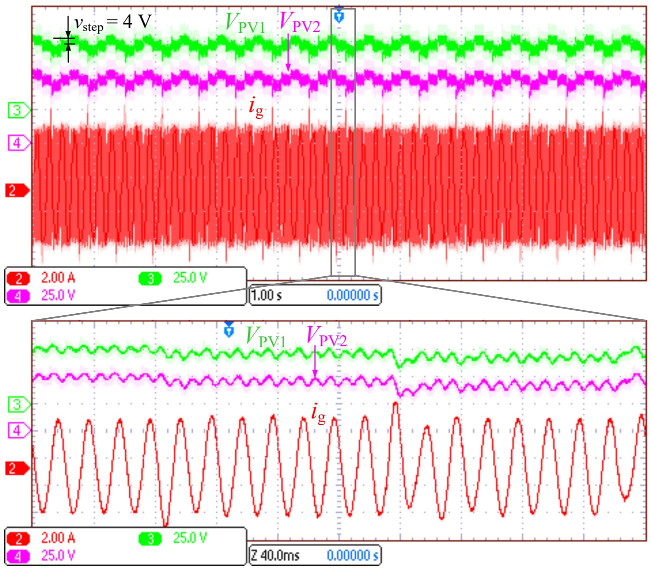

Fig. 9. Experimental results of a CHB PV inverter with two cascaded PV converter cells, operated at 200 W/m^2 and 25 °C. (V_{PV1} [25 V/div] and V_{PV2} [25 V/div]: DC voltages for cell #1 and #2; i_g [2 A/div]: grid current).

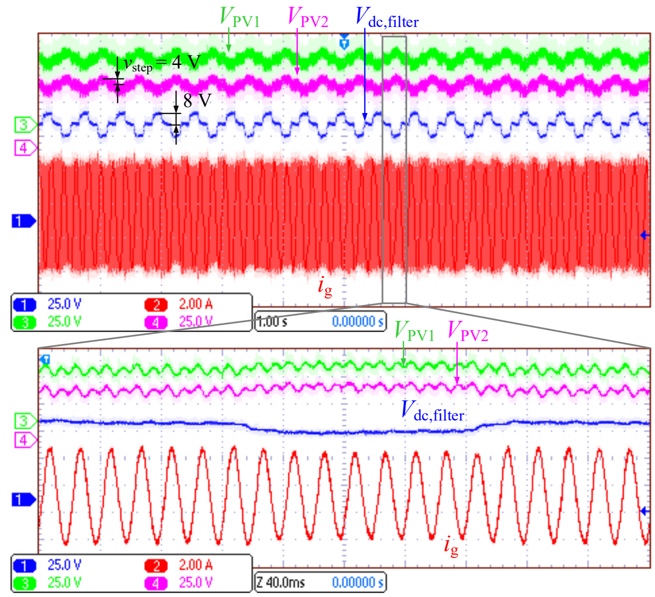

Fig. 11. Experimental results of a CHB PV inverter with two PV converter cells and one cascaded interharmonic filter cell, operated at 200 W/m^2 and 25 °C. (V_{PV1} [25 V/div], V_{PV2} [25 V/div] and $V_{dc,filter}$ [25 V/div]: DC voltages for cell #1, #2 and #3; i_g [2 A/div]: grid current).

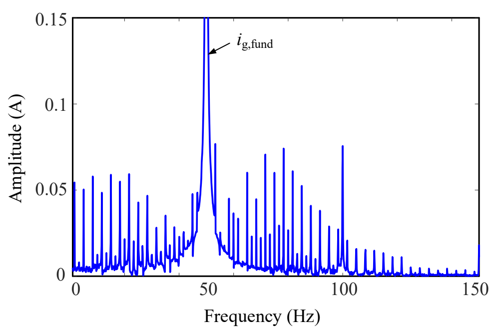

Fig. 10. Frequency spectrum of the grid current shown in Fig. 9.

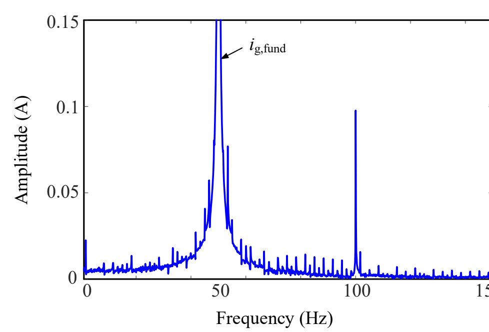

Fig. 12. Frequency spectrum of the grid current shown in Fig. 11.

when the sum of PV voltages has a lower oscillation amplitude. Thus, it is also suggested to equip the interharmonic filter with the PS-MPPT control in [13]. In steady state, the PS-MPPT is capable to suppress the interharmonics to a large extent. Then, with the employment of the interharmonic filter, the interharmonics will be further suppressed, especially for CHB PV inverters with an odd number of cells. On the other hand, during varying environmental conditions, the interharmonic suppression performance for the PS-MPPT may be limited [14]. In this case, the interharmonics can still be effectively suppressed with the interharmonic filter, since the DC voltage of the interharmonic filter can always be controlled in a way to keep the equivalent total DC voltage constant, and thereby preventing from the generation of interharmonics in the primary control loops. Therefore, the interhamonic suppression performance can be enhanced by the proposed interharmonic filter for CHB PV inverters with the PS-MPPT control.

B. *Experimental Results*

To further validate the effectiveness of the proposed method, experiments have been conducted on a down-scaled CHB PV inverter, as shown in Fig. 8, with cell #1 and #2 interfaced with PVs, which are emulated by Keysight E4360A PV simulator, and cell #3 performs as the interharmonic filter. A TMS320F28335 digital signal processor was employed to implement the control algorithms, and an Infineon FS50R12KT4_B15 IGBT module was adopted for each converter cell. Experimental parameters are the same with the simulations, except that: 1) the rated PV power for each converter cell is reduced to 300 W, 2) the grid voltage is reduced to 40 V(rms) due to the limited output voltage of the PV simulator, 3) the MPPT step-size and perturbation frequency are reduced to 4 V and 6.67 Hz, respectively.

Firstly, the experimental results for the 2-cell CHB PV inverter without the interharmonic filter is shown in Fig. 9. As observed in Fig. 9, the DC voltages of the two cells were oscillating in-phase, with their oscillation amplitudes being 4 V. As a result, periodical spikes appeared in the grid current, as shown in the zoomed-in plot in Fig. 9, and the fast Fourier transform (FFT) results shown in Fig. 10 confirm that there were a large amount of interharmonics, with the amplitudes of the dominant inter-harmonics being around 0.05 A. On the other hand, as shown in Fig. 11, after the employment of the interharmonic filter (cell #3), an 8-V oscillating voltage is generated by the proposed series filter to counteract with the in-phase DC voltage oscillations of the two PV cells. The total DC voltage reference was maintained constant at 168 V, and the DC voltage of the interharmonic filter was thus oscillating around 75 V. With the proposed method, the amplitude of the grid current became more stable, as shown in the zoomed-in plot in Fig. 11, and consequently, interharmonics were significantly suppressed, as shown in the frequency spectrum in Fig. 12. Therefore, the proposed method can effectively suppress interharmonics from CHB PV inverters.

IV. Conclusion

To suppress interharmonics from the CHB PV inverters, a series interharmonic filter was proposed in this paper. By controlling the DC voltage of the interharmonic filter in a way to counteract with the oscillations of PV converter cells, the equivalent total DC voltage can be kept constant, and the interharmonics in the grid current can be significantly reduced. Moreover, in practice, the interharmonic filter cell can be reserved as a redundant cell, or selected from existing PV converter cells. Furthermore, the proposed interharmonic filter can also be equipped with the PS-MPPT method to enhance the interharmonic suppression performance in both steady-state and dynamic conditions. Simulation and experimental results presented in this paper have confirmed the effectiveness of the proposed solution to address the interharmonic issue.

References

[1] V. Ravindran, T. Busatto, S. K. Ronnberg, J. Meyer, and M. Bollen, "Time-varying interharmonics in different types of grid-tied PV inverter systems," *IEEE Trans. Power Del*., vol. 35, no. 2, pp. 483-496, Apr. 2020.

[2] *IEEE Standard for Interconnection and Interoperability of Distributed Energy Resources with Associated Electric Power Systems Interfaces*, IEEE Standard 1547-2018, Apr. 2018.

[3] *Grid code compliance assessment methods for grid connection of wind and PV power plants*, Ed. 1, IEC/TS 63102, 2016.

[4] V. Ravindran, S. K. Rönnberg, and M. H. J. Bollen, "Interharmonics in PV systems: a review of analysis and estimation methods; considerations for selection of an apt method," *IET Renew. Power Gener*., vol. 13, no. 12, pp. 2023–2032, Sept. 2019.

[5] A. Sangwongwanich, Y. Yang, D. Sera, H. Soltani, and F. Blaabjerg, "Analysis and modeling of interharmonics from grid-connected photovoltaic systems," *IEEE Trans. Power Electron*., vol. 33, no. 10, pp. 8353-8364, Oct. 2018.

[6] C. Hou, M. Zhu, Z. Li, Y. Li and X. Cai, "Inter-harmonic THD amplification of voltage source converter: concept and case study," *IEEE Trans. Power Electron.*, DOI: 10.1109/TPEL.2020.2994751.

[7] A. Sangwongwanich, Y. Yang, D. Sera, and F. Blaabjerg, "Interharmonics from grid-connected PV systems: mechanism and mitigation," in *Proc. 2017 IEEE 3rd Int. Future Energy Electron. Conf. (IFEEC-ECCE Asia)*, Jun. 2017, pp. 722–727.

[8] A. Sangwongwanich and F. Blaabjerg, "Mitigation of interharmonics in PV systems with maximum power point tracking modification," *IEEE Trans. Power Electron*., vol. 34, no. 9, pp. 8279-8282, Sept. 2019.

[9] J. He, Y. Li, C. Wang, Y. Pan, C. Zhang, and X. Xing, "Hybrid microgrid with parallel- and series-connected microconverters," *IEEE Trans. Power Electron*., vol. 33, no. 6, pp. 4817-4831, Jun. 2018.

[10] X. Zhang, Y. Hu, W. Mao, T. Zhao, M. Wang, F. Liu, and R. Cao, "A grid-supporting strategy for cascaded H-bridge PV converter using VSG algorithm with modular active power reserve," *IEEE Trans. Ind. Electron*., DOI: 10.1109/TIE.2019.2962492.

[11] Y. Pan, A. Sangwongwanich, Y. Yang, and F. Blaabjerg, "A phase-shifting MPPT method to mitigate interharmonics from cascaded H-bridge PV inverters," in *Proc. IEEE APEC Expo*., Mar. 2020, pp. 157-163.

[12] S. Kouro, P. Lezana, M. Angulo and J. Rodriguez, "Multicarrier PWM with DC-link ripple feedforward compensation for multilevel inverters," *IEEE Trans. Power Electron*., vol. 23, no. 1, pp. 52-59, Jan. 2008.

[13] Y. Pan, A. Sangwongwanich, Y. Yang and F. Blaabjerg, "A phase-shifting MPPT to mitigate interharmonics from cascaded H-bridge PV inverters," *IEEE Trans. Ind. Appl*., DOI: 10.1109/TIA.2020.3000969.

[14] Y. Pan, A. Sangwongwanich, Y. Yang, and F. Blaabjerg, "A random sampling-rate MPPT method to mitigate interharmonics from cascaded H-bridge photovoltaic inverters," in *Proc. 2020 IEEE 9th Int. Power Electron. Motion Control Conf. (IPEMC-ECCE Asia)*, Nov. 2020, pp. 1-6.

[15] Y. Pan, C. Zhang, S. Yuan, A. Chen and J. He, "A decentralized control method for series connected PV battery hybrid microgrid," in *Proc. IEEE Transp. Electrific. Conf. Expo, Asia-Pacific (ITEC Asia-Pacific)*, Harbin, China, Aug. 2017, pp. 1–6.

[16] Y. Ko, M. Andresen, G. Buticchi and M. Liserre, "Power routing for cascaded H-bridge converters," *IEEE Trans. Power Electron.*, vol. 32, no. 12, pp. 9435-9446, Dec. 2017.

[17] T. Zhao, X. Zhang, W. Mao, M. Wang, F. Wang, X. Wang, and J. Xu. "Harmonic compensation strategy for extending the operating range of cascaded H-bridge PV inverter," *IEEE J. Emerg. Sel. Topics Power Electron.*, vol. 8, no. 2, pp. 1341-1350, Jun. 2020.

[18] E. Jacobsen and R. Lyons, "The sliding DFT," *IEEE Signal Process. Mag*., vol. 20, no. 2, pp. 74–80, Mar. 2003.

[19] G. Konstantinou, J. Pou, S. Ceballos and V. G. Agelidis, "Active redundant submodule configuration in modular multilevel converters," *IEEE Trans. Power Del*., vol. 28, no. 4, pp. 2333-2341, Oct. 2013.